CHEMISTRY
AN ASIAN JOURNAL

DOI: 10.1002/asia.201100903

Reactivity of Bispropargyl Sulfones under Basic Conditions: Interplay Between Garratt–Braverman and Schmittel/Myers–Saito Cyclization Pathway

Raja Mukherjee,[a] Sayantan Mondal,[a] Amit Basak,*[a] Dibyendu Mallick,[b] and Eluvathingal D. Jemmis*[b, c]

Abstract: The preference for Garratt–Braverman (GB) over Myers–Saito (MS) and Schmittel (SCM) cyclizations has recently been demonstrated in sulfones capable of undergoing all three of the processes. As the GB cyclization is a self-quenching process, there is a need to change the selectivity to the non-self-quenching MS or SCM pathway so as to enhance the DNA-cleaving efficiency that operates through the radical-mediated process. Herein we report a conformational constraint-based strategy developed by using computations (M06-2X/6-31+G*) to switch the selectivity from GB to MS/SCM pathway which also results in greater DNA-cleavage activity. The preference for GB could be brought back by easing the constraint with the help of spacers.

Keywords: antibiotics · cyclization · DNA cleavage · enediyne · sulfones

Introduction

The discovery of naturally occurring and highly potent anticancer agents collectively called enediyne antibiotics[1] in the 1980s triggered the search for ways to spontaneously generate diradicals.[2] Since then, the role of the diradicals in organic synthesis,[3] in the preparation of new materials,[4] and especially in pharmacology[5] has become a major topic of research interest. The conditions to generate diradicals and their efficiency of hydrogen abstraction vary widely. Diradicals that do not have any mechanism to self-quench become diamagnetic by means of abstraction of atoms from external sources. Bergman cyclization (BC)[6] and related reactions like Myers–Saito (MS)[7] and Schmittel (SCM)[8] belong to this category (Scheme 1). On the other hand, cyclizations like Garratt–Braverman (GB)[9] that involve conjugated bisallenes have a self-quenching mechanism; therefore chances of interaction of the diradicals with external sources are greatly reduced. Although the DNA cleavage exhibited by these molecules may also involve Michael addition of DNA base followed by Maxam–Gilbert-type cleavage,[10] the cleaving efficiency of these molecules is generally much less[11] than molecules that undergo BC or MSC. The efficiency of hydrogen abstraction by a diradical is of utmost importance from a medicinal chemistry standpoint because that will finally decide the potential of the diradical-generating molecule as an antitumor agent. Recently[11] we have shown the complete preference for GB over MS/SCM in bispropargyl sulfones, which have the possibility to undergo all three processes under basic conditions. This preference for GB makes these molecules less efficient as DNA-cleaving agents. It would be better if it were possible to reverse the preference for the cyclization processes. In this paper, we demonstrate a conformational constraint-based strategy by which one can completely shift the preference of cycloaromatization from GB to the MS or SCM pathway in bispropargyl sulfones. We have also demonstrated that the preference for GB could be brought back through incorporation of spacers to lessen the constraint.

[a] R. Mukherjee, S. Mondal, Dr. A. Basak
Department of Chemistry,
Indian Institute of Technology
Kharagpur 721 302 (India)
E-mail: absk@chem.iitkgp.ernet.in

[b] D. Mallick, Dr. E. D. Jemmis
Department of Inorganic and Physical Chemistry
Indian Institute of Science
Bangalore 560 012 (India)

[c] Dr. E. D. Jemmis
Indian Institute of Science Education and
Research Thiruvananthapuram, CET Campus
Thiruvananthapuram, 695016, Kerala (India)
E-mail: jemmis@iisertvm.ac.in

Supporting information for this article is available on the WWW under http://dx.doi.org/10.1002/asia.201100903.

Results and Discussion

Experimental Studies

Initially, we had two strategies in mind to switch the preference. Both strategies aimed to prevent the molecule from adapting the conformation suitable for the GB pathway, either by steric effects or through geometric constraints. In the first strategy, we argued that the intermediates for GB

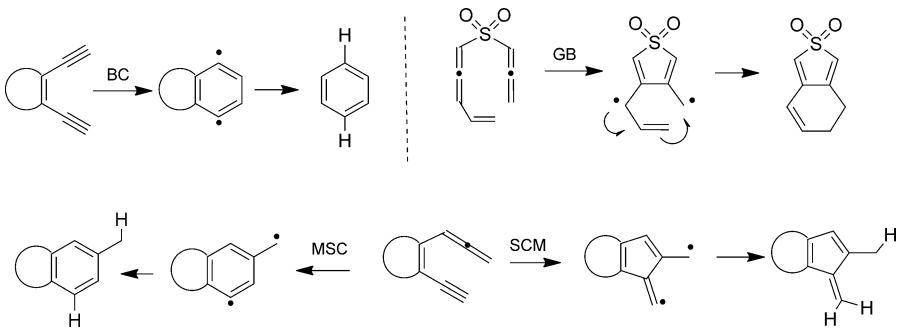

Scheme 1. Various cyclization pathways in the presence of hydrogen donors.

cyclization, namely **3** and **5**, will be destabilized by possible steric repulsions as shown in Scheme 2. Moreover, phenyl-substituted eneyne allenes are known[12] to undergo SCM cyclization because of the extra stability of the benzylidene radical **4** (Scheme 2). However, when the phenyl-substituted

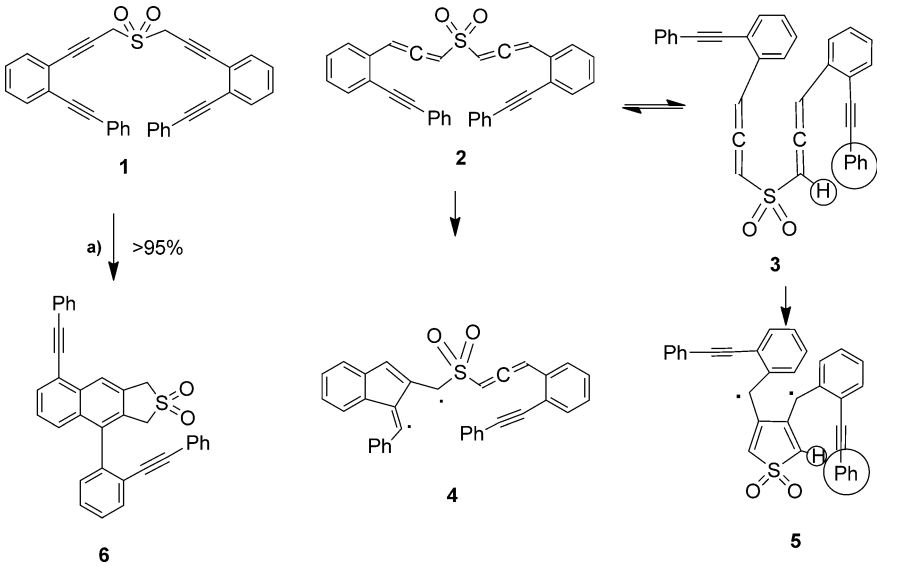

Scheme 2. The proposed steric crowding for the GBC intermediates and reactivity of sulfone **1**. Reaction condition a) dry Et_3N, 45 min.

bispropargyl sulfone **1** (for its synthesis, see the Supporting Information) was treated with a base, the only product isolated, in a very high yield, was the GB product **6** (Scheme 2). Thus, neither the expected steric crowding as in **3** and **5** nor the extra stability of biradical **4** changed the course of the reaction. Computational studies, described later, at the B3LYP/6-31G* level indicated the preference of GB product, as has also been observed earlier.[11] Like the previously reported sulfones, the higher thermodynamic stability of the initially formed GB biradical over MS biradical and the intramolecular self-quenching nature of the GB pathway remain the main reasons for this preference (see the Supporting Information for a detailed discussion).

The second strategy involved tying up the two ends of the alkyne by oxidative coupling. If the compound has to undergo GB cyclization, it has to adapt the conformation **M** (Scheme 3), which is 12.0 kcal mol^{-1} higher in energy at the M06-2X/6-31+G* level of theory[20] than the initial conformation required for MS or SCM cyclization. The conformation for the diradical is then best represented by **N**. In comparison to the diradical **P** formed by the MS pathway, **N** is 3.6 kcal mol^{-1} less stable and also not in a position to undergo the self-quenching process that is essential to lead to the finally stable GB product. The conformation **O**, through which self-quenching can occur, is extremely distorted and could not be obtained as stationary point computationally. However, alternate MS or SCM cyclization pathways were calculated to be feasible (see below).

With this idea in mind, we proceeded with the synthesis of the target sulfones **7** and **8**. The key steps involved are the Cu^I-catalyzed modified Glaser coupling[13] of the terminal alkynes **10** and **15** followed by intramolecular cyclic sulfide formation. Oxidation with *meta*-chloroperoxybenzoic acid (*m*-CPBA) finally led to the starting sulfones **7** and **8** (Schemes 4 and 5). The experiment was first carried out with the aromatic sulfone **7**. Thus the compound dissolved in $CHCl_3$ was treated with triethylamine (TEA, 1 equiv) and 1,4-cyclohexadiene

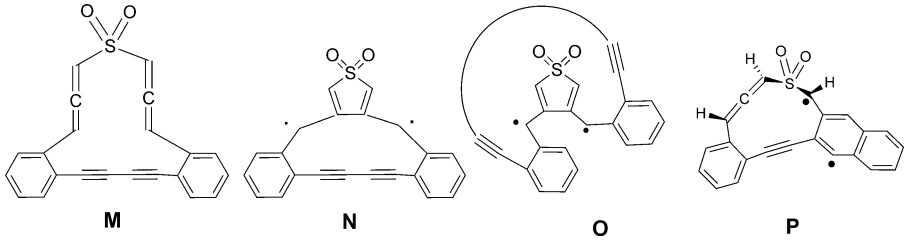

Scheme 3. The possible intermediates for GBC from a conformationally constrained sulfone.

CHEMISTRY
AN ASIAN JOURNAL

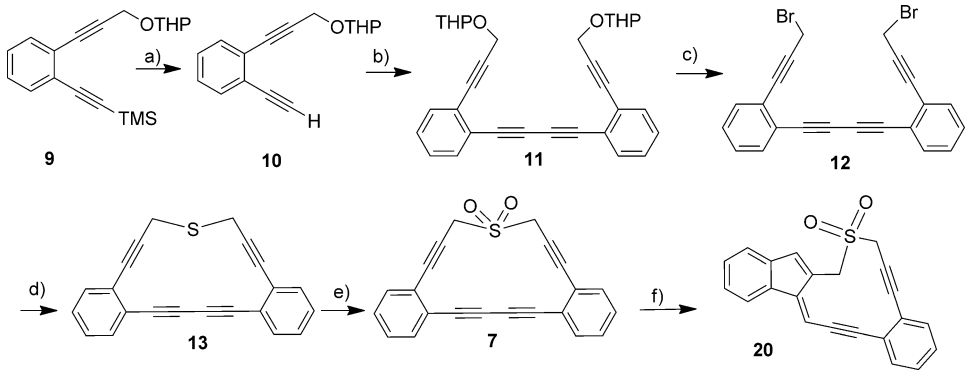

Scheme 4. Synthesis and reactivity of sulfone **7**. Reaction conditions: a) KF, dry MeOH, 4 h (95 %); b) DBU, CuBr, O_2, dry pyridine, 4 h (78 %); c) PPTS, EtOH, 55 °C, 5 h; MsCl, Et_3N, 0 °C, 10 min; LiBr, dry THF, 6 h (91 %); d) Na_2S, TBAB, THF/H_2O, 0 °C, 30 min (82 %); e) mCPBA, dry DCM, rt, 1h (89 %); f) 1,4-CHD, Et_3N, 24 h (32 %). DBU = 1,8-diazabicyclo[5.4.0]undec-7-ene.

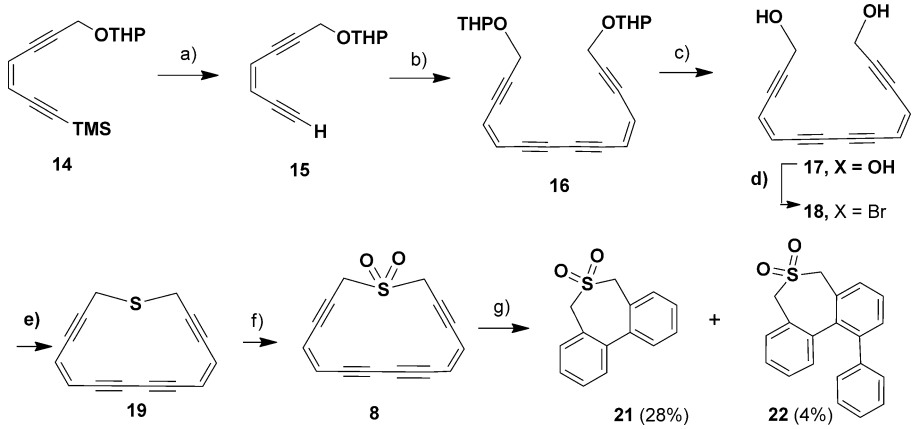

Scheme 5. Synthesis and reactivity of sulfone **8**. Reaction conditions: a) KF, dry MeOH, 4 h (91 %); b) DBU, CuBr, O_2, dry pyridine, 4 h (71 %); c) PPTS, EtOH, 55 °C, 5 h (92 %); d) MsCl, Et_3N, 0 °C, 10 min; LiBr, dry THF, 6 h (81 %); e) Na_2S, TBAB, THF/H_2O, 0 °C, 30 min (72 %); f) mCPBA, dry DCM, rt, 1 h (90 %); g) 1,4-CHD, Et_3N, dry benzene, 24 h

(1,4-CHD, 10 equiv).[14] Within 1 hour, the substrate completely disappeared and from the reaction mixture only a single product could be isolated, the structure of which was found to be **20** by NMR spectroscopy and mass spectrometric data. The structure was further confirmed by single-crystal X-ray analysis (ORTEP diagram shown in Figure 1).[15] As expected, no GB product could be isolated from the reaction mixture. The formation of **20** can only be explained by the initial isomerization to the monoallene followed by Schmittel cyclization (Scheme 4). The low yield of **20** (only 32 %) was due to extensive polymerization of the intermediate biradicals.

The aliphatic sulfone **8**, on the other hand, upon similar base treatment produced two products (one major **21** along with the minor product **22**) identified by NMR spectroscopy and mass spectral data. In the major product **21**, the ^{1}H NMR spectrum shows only one singlet for the two methylenes, thus indicating the symmetrical nature of the structure. In addition, the ^{13}C NMR spectrum showed a complete absence of the acetylenic carbon atoms in the range of $\delta =$ 80–110 ppm. The spectral data also completely matched with what has been reported in the literature.[16] The formation of **21** can be explained through formation of monoallene followed by MS cyclization and quenching by H from 1,4-CHD and repetition of the same sequence. The alternative possibility of involvement of a bisallene can be ruled out because that would involve a tetraradical.[17] The minor product could have originated through the attack of the benzene radical formed in the MSC to a benzene molecule. Semmelhack et al.[18] had previously reported the formation of a product that arose out of similar trapping with a phenyl radical.

Now that we were able to switch the preference from GB to SCM or MS, these sulfones were expected to show better DNA-cleavage activity than that for earlier reported[11] similar compounds that undergo GB cyclization. Thus the sulfones **7** and **8** were incubated with pBR322 DNA at pH 8.5. Aliquots were taken at 12, 24, and 48 hours and subjected to agarose gel electrophoresis. The results demonstrated that both sulfones have cleavage activity (Figure 2). Although the cleavage efficiency of the aromatic sulfone **7** did not improve much, the aliphatic sulfone **8** showed much stronger DNA-cleaving activity (72 % at 20 μM relative to 10 % at 1 mM for acyclic sulfones as already reported[11]).

To lend further support to the fact that conformational constraints play a major role in the above switch from GB to MSC or SCM, we prepared a series of sulfones **30a–d** with increasing degrees of constraints from $n = 4$ to $n = 1$. This was done by varying the length of the spacer between the acetylenic carbon atoms to alter the steric constraint. When these sulfones were separately treated with Et_3N in $CDCl_3$, compounds **30a–c** with spacers of $n = 4$, 3, and 2 gave exclusively GB products, whereas for compound **30d** with spacer $n = 1$, we could not isolate any well-defined product (Scheme 6). However, the ^{1}H NMR spectrum of the crude reaction mixture ruled out the formation of any GB product. The results showed that once the steric strain was removed as in compounds **30a–c**, the preference to undergo GBC was brought back. For compound **30d**, because of the

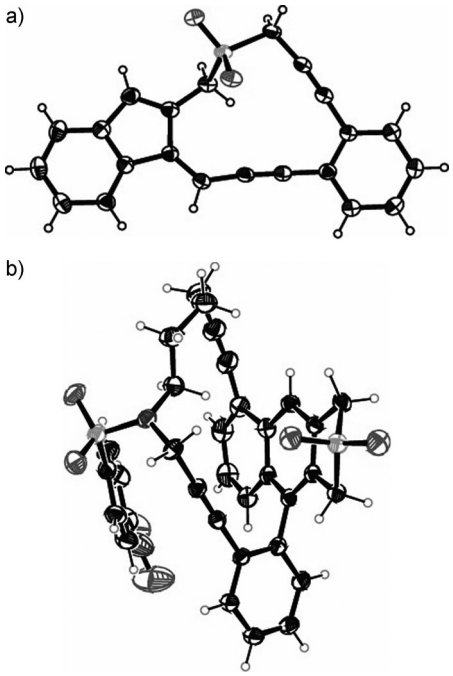

Figure 1. X-ray structures of a) **20** and b) **32a**.

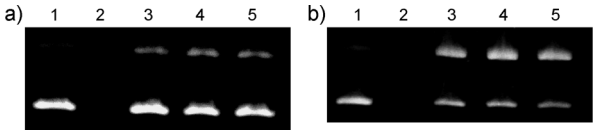

Figure 2. DNA-cleavage studies with the sulfones at 37 °C: a) lane 1: DNA (7 μL) in tris(hydroxymethyl)aminomethane (Tris)-acetate buffer containing ethylenediaminetetraacetic acid (EDTA; TAE buffer, pH 8.5, 5 μL) and DMSO (5 μL); lanes 3–5: DNA (7 μL) in TAE buffer (5 μL) + sulfone **7** in DMSO (20 μM) after incubation for 12, 24, and 48 h, respectively. Cleavage as determined by densitometric analysis: lane 1: 4%, lane 3: 31%, lane 4: 32%, lane 5: 35%. b) lane 1: DNA (7 μL) in TAE buffer (5 μL) + DMSO (5 μL); lanes 3–5: DNA (7 μL) in TAE buffer (5 μL) + sulfone **8** in DMSO (20 μM) after incubation for 12, 24, and 48 h, respectively. Cleavage as determined by densitometric analysis: lane 1: 3%, lane 3: 58%, lane 4: 67%, lane 5: 72%. The upper band in both gels corresponds to supercoiled DNA, while the lower band corresponds to nicked DNA. Lanes 2, blank.

short spacer length, the steric strain for attaining the conformation for BC prevented the molecules from undergoing such a process. Computational exercises (discussed later) also supported such results. The structures of the GB products were characterized by NMR spectroscopy and mass spectroscopy, and from the X-ray crystal structure of one of the products (Figure 1).

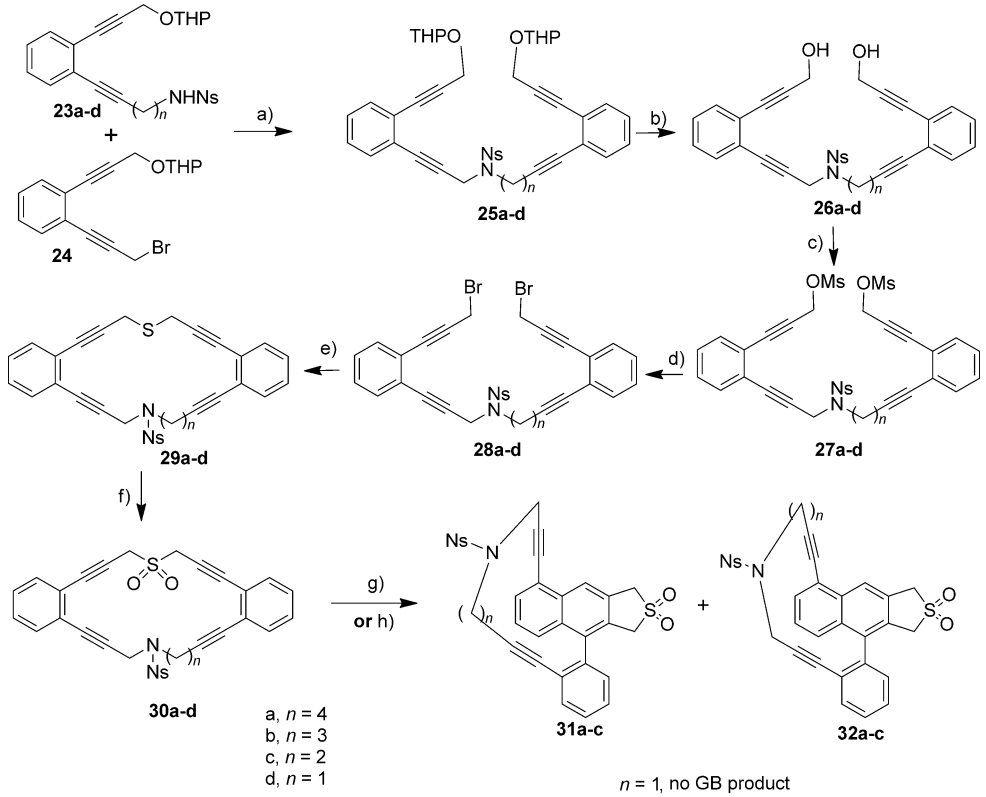

Scheme 6. Synthesis and reactivity of sulfones **30a–d**. Reaction conditions: a) K_2CO_3, DMF (>90 %); b) PPTS, EtOH, 50 °C (>85 %); c) MsCl, Et_3N, DCM, 0 °C (>95 %); d) LiBr, THF (>90 %); e) Na_2S, THF/H_2O (>75 %), TBAB, 0 °C→rt (>90 %); f) mCPBA, DCM, 0 °C→R.T. (72 %); g) Et_3N, $CDCl_3$ (>90 %); h) Et_3N, 1,4-CHD, $CDCl_3$ (>90 %).

CHEMISTRY
AN ASIAN JOURNAL

Computational Study

The strategy based on conformational constraints to switch the preference from GB cyclization to the MS or SCM mode was computationally analyzed.[19–23] As we mentioned earlier, the non-occurrence of GB cyclization for one of the conformationally constrained molecule **7** is due to the instability of the initial biradical **M** compared to that of MS or SCM biradical (**MS-DR** and **SCM-DR**), and more importantly, because of its inability to undergo self-quenching process due to the geometrical constraints. After successfully explaining the non-occurrence of the GB reaction for the geometrically constrained sulfone **7**, we searched for an explanation for the double occurrence of the MS pathway for aliphatic sulfone **8** as opposed to the occurrence of an SCM pathway for the corresponding aromatic sulfone **7**. The reaction profile for the aliphatic sulfone **8** was studied in detail at the M06-2X/6-31+G* level of theory[20,22] by using the Gaussian 09 package[19] (Figure 3). We took bisallenic sulfone (**SM1**) as a starting material, which can be obtained by the isomerization of sulfone **8** under basic conditions. This bisallenic sulfone can undergo either MS cyclization or SCM cyclization or both. There is a slight difference in energy between the initial biradicals (**MS1** and **SCM1**) for the two reactions ($\Delta G_{MS1-SCM1} = -0.7$ kcal mol^{-1}). The activation energy required for the formation of the **MS1** biradical is 26.1 kcal mol^{-1}, whereas that for the formation of **SCM1** is 27.6 kcal mol^{-1}. Hence the biradical **MS1** is thermodynamically slightly more stable and its formation is also kinetically more feasible. To understand the solvent effects on the reaction rates and selectivities, we have carried out the calculations in $CHCl_3$. We have found that the increase in the free-energy difference ($\Delta\Delta G^{\neq}$) between the two transition states (**TS1-MS** and **TS1-SCM**) from 1.5 kcal mol^{-1} in the gas phase to 2.0 kcal mol^{-1} in $CHCl_3$ makes the formation of the **MS1** biradical more favorable. We have not observed any other significant changes in the relative free energies of the different species involved in the reactions in $CHCl_3$ from their gas-phase values (Figure 3). After the formation of the biradical, it abstracts hydrogen from 1,4-CHD, which is present in the reaction medium. The activation energy for the first hydrogen-abstraction step for the MS pathway is 4.6 kcal mol^{-1}, whereas that of the SCM pathway is 8.0 kcal mol^{-1} (Schemes S3 and S4 in the Supporting Information). This implies that, after the formation of biradical **MS1**, it is readily converted to the single cyclization product **MS2**. We have found a very high thermodynamic stability of the hydrogen-quenched species **MS2** over **SCM2** ($\Delta G_{MS2-SCM2} = -28.4$ kcal mol^{-1}), and this can be attributed to the aromatic stabilization gained by the formation of a phenyl ring in the case of **MS2**. So for the aliphatic sulfone, MS cyclization is preferred due to the lower kinetic barrier for the formation of the initial biradical and its facile conversion to the product with lower hydrogen abstraction barrier than those of the SCM pathway.

We also chose a bisallenic sulfone as the starting material for aromatic sulfone **7**. For **7**, the preference for SCM cyclization over MS cyclization happens on account of the higher kinetic and thermodynamic stability of the Schmittel biradical (**SCM-DR**) over the Myer–Saito biradical (**MS-DR**, Figure 4). The biradical **SCM-DR** is 1.8 kcal mol^{-1} more stable than the diradical **MS-DR**. The activation energy barrier for the biradical generation process is less (35.8 kcal mol^{-1}) for the Schmittel reaction than that of the MS reaction (37.7 kcal mol^{-1}). Hence the biradical **SCM-DR** is thermodynamically and kinetically more stable than the **MS-DR** biradical, which in turn causes the preference for SCM over MS. Then the biradicals are quenched by abstracting hydrogen from 1,4-CHD, and finally they isomerize to the final products. Unlike the aliphatic sulfone for which we have observed double cyclization, the aromatic sulfone shows only single cyclization. This may be due to the fact that the SCM

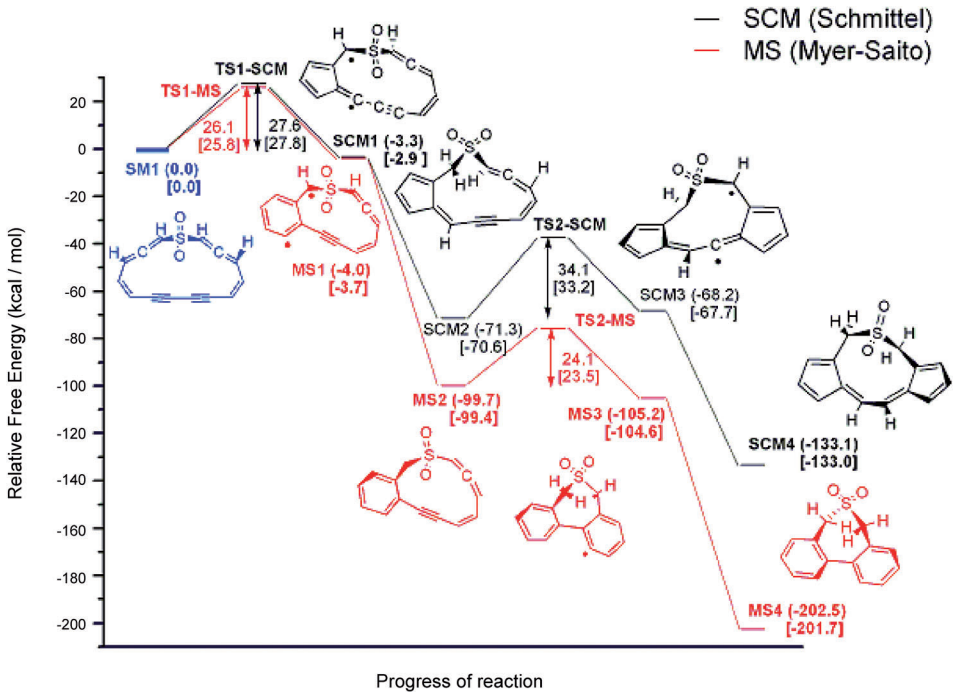

Figure 3. Comparison between Myer–Saito (MS) and Schmittel (SCM) reaction pathways for aliphatic systems. The relative free energies (ΔG_{298K}) in the gas phase were calculated at the M06-2X/6-31+G* level of theory (values within square brackets were calculated in $CHCl_3$) for different species involved in the reaction pathway.

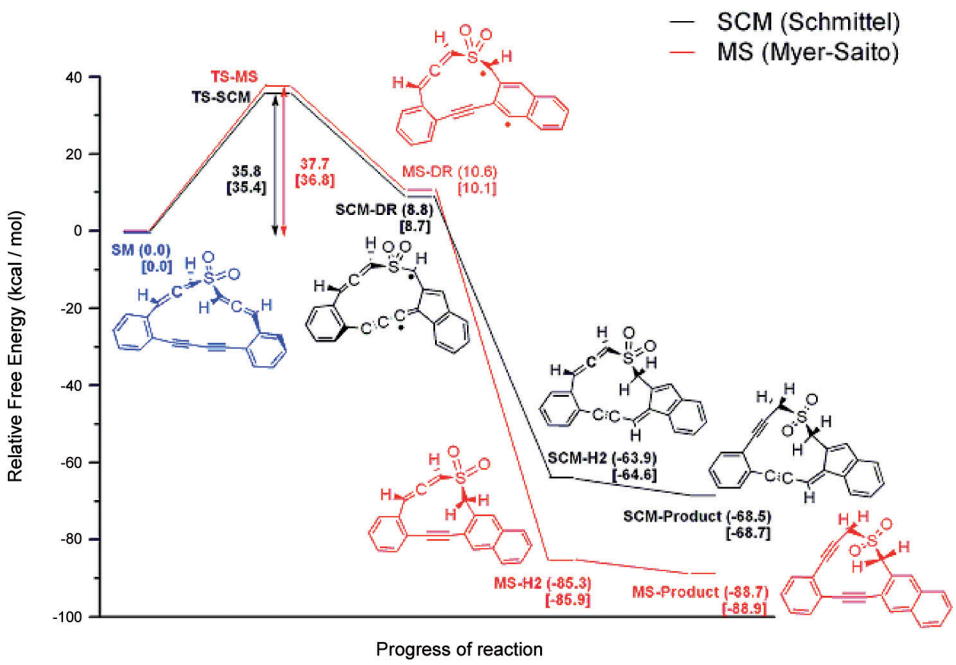

Figure 4. Comparison between Myer–Saito (MS) and Schmittel (SCM) reaction pathways for aromatic systems. The relative free energies (ΔG_{298K}) in the gas phase were calculated at the M06-2X/6-31+G* level of theory (values within square brackets were calculated in $CHCl_3$) for different species involved in the reaction pathway.

biradical produced after the first cyclization cannot be stabilized through extended conjugation, which is lost after the first cyclization.

We have also calculated the activation energies and the reaction free energies for Garratt–Braverman and Myer–Saito reactions for different spacer lengths ($n=3$, 2, 1). To reduce the computational cost, we have replaced the nosyl (Ns) group with hydrogen in all these species. For all the cases, the initial conformations for the GB pathway are found to be more stable than that for the MS pathway (Table 1). The free-energy differences (ΔG_{GB-MS}) between the initial conformations for GB and MS reactions are −6.4, −5.0, and −3.0 kcal mol^{-1} for $n=3$, 2, and 1, respectively. From Table 1 it is evident that as the spacer length increases, the GB cyclization becomes more and more favorable (along with an increase in the reaction rate) to the MS cyclization. These results are highly consistent with the experimentally observed data.

Table 1. Computed activation and reaction free energies [kcal mol^{-1}] for Garratt–Braverman and Myer–Saito reactions at the M06-2X/6-31+G* level of theory for different spacer lengths (Scheme 5).

Spacer length	ΔG_{GB-MS}[a]	Garratt–Braverman cyclization		Myer–Saito cyclization	
		$\Delta^{+}G_{298K}$	ΔG_{298K}	$\Delta^{+}G_{298K}$	ΔG_{298K}
$n=3$	−6.4	25.8	−3.9	32.2	8.9
$n=2$	−5.0	22.8	−4.8	24.3	−0.5
$n=1$	−3.0	22.2	−4.5	24.6	−0.6

[a] Free-energy difference between the initial conformations for GB and MS reactions.

Conclusion

In conclusion, we have been successful in executing a strategy to interchange the preference of cyclization of suitably substituted bispropargyl sulfones between the diradical self-quenching GB mode and the externally quenched MS or SCM pathway by incorporation of a steric constraint of varying degree. The experimental results also fit nicely with the theoretical calculations. The findings should provide a new twist in the design of radical mediated DNA-cleaving agents and also in synthesis.

Experimental Section

Computational Details

All the computations were performed with the Gaussian 09 software package.[19] Optimization of all ground-state geometries except phenyl-substituted systems were done using the M06-2X functional,[20] which accounts for the dispersive interaction. Like the previously reported work,[11] the B3LYP functional[21,22] was used for the phenyl-substituted system. The 6-31+G* basis set was used for all the calculations. The stability of the wave function was checked for all the species. A restricted approach was used in the computational analysis for the closed-shell structures, whereas an unrestricted broken-spin symmetry approach (BS-UM06-2X) was used for the open-shell singlet-state transition states and intermediates. The broken-spin symmetry solutions were achieved by feeding the SCF computation with a 50:50 mix (singlet/triplet) initial guess of the HOMO and LUMO orbitals.[23a] This approach worked acceptably well for the biradical intermediates and the transition states of GB reaction. But for the MS biradicals this approach is problematic, because the HOMO and LUMO for these biradicals do not correspond to the orbitals required for proper mixing. In these cases we used PO-DFT, suggested by Cremer and co-workers,[24] to calculate the open-shell singlet state. The nature of stationary points was characterized by vibrational frequency calculation.

Characterization

All ^{1}H and ^{13}C NMR spectra were respectively recorded at 400 and 100 MHz in $CDCl_3$ unless mentioned otherwise. The X-ray crystal data was recorded with a Bruker AXS Smart Apex-II. ESI-MS and HRMS were taken with a Waters LCT mass spectrometer; the solutions of the compounds were injected directly into the spectrometer by means of a Rheodyne injector equipped with 10 μL loop. A Phoenix 20 micro LC syringe pump delivered the solution to the vaporization nozzle of the electrospray ion source at a flow rate of 3 μL min^{-1}. Nitrogen was used both as a drying gas and for nebulization with flow rates of approximately 3 L min^{-1} and 100 mL min^{-1}, respectively. Pressure in the analyzer region was usually about 3×10^{-5} torr.

General Procedure for the Glaser Coupling

The terminal alkyne (2 mmol) was dissolved in dry pyridine (15 mL) and 1,8-diazabicyclo[5.4.0]undec-7-ene (DBU) and CuBr (5 mol% of each) were added to it. Then oxygen gas was slowly and continuously bubbled through the reaction for 4 h. The reaction mixture was then poured into

ice-cold 3 N HCl (25 mL) and was extracted with CH_2Cl_2 (3×25 mL). The combined organic layers were dried over anhydrous sodium sulfate and CH_2Cl_2 was evaporated under vacuum. The coupling product was purified by column filtration with ethyl acetate/petroleum ether as eluent.

General Procedure for THP Deprotection

The THP-protected alkynyl compound (1 mmol) and a catalytic amount of pyridinium *p*-toluenesulfonate (PPTS; 5 mol%) was stirred in ethanol (10 mL) at 55 °C for 6 h. Ethanol was removed, and the crude mixture was directly subjected to column chromatography for purification.

General Procedure for Mesylation and Bromide Formation Reaction

The alcohol (0.4 mmol) was treated with triethylamine (2 equiv) and mesyl chloride (2 equiv) in dry dichloromethane (5 mL) at 0 °C under an argon atmosphere until TLC showed the disappearance of the starting material. The reaction was quenched by the addition of brine and extracted with CH_2Cl_2 (20 mL). The organic layer was dried with anhydrous sodium sulfate. The solvent was evaporated, and the product, mesylate, was vacuum-dried. LiBr (2 equiv) was added to the crude mesylate (0.3 mmol) in dry THF (5 mL) and stirred for 2 h after the completion of the reaction. Removal of solvent followed by silica gel column filtration with ethyl acetate/hexane afforded the pure bromide.

General Procedure for the Synthesis of SulfideMethod A for the Cyclic Sulfide

The cyclic sulfide was synthesized according to a high-dilution technique. The bromide (0.1 mmol) was dissolved in THF (34 mL) and stirred at 0 °C. Sodium sulfide (0.5 equiv) was added, followed by catalytic amount of tetrabutylammonium bromide (TBAB, 2 mol%) and water (0.5 mL). The reaction mixture was stirred at room temperature until TLC showed disappearance of the bromide. The reaction mixture was then partitioned between EtOAc and water. The organic layer was dried over anhydrous sodium sulfate. The solvent was evaporated under vacuum and the product was purified by silica gel column chromatography with hexane/ethyl acetate as eluent.

Method B for the Open-Chain Sulfide

The bromide (0.1 mmol) was dissolved in dry methanol (5 mL) and stirred at 0 °C. Sodium sulfide (0.5 equiv) was added. The reaction mixture was allowed to stir at room temperature until TLC showed disappearance of the bromide. Methanol was evaporated off. The crude was subjected to silica gel column chromatography for isolation.

General Procedure for Oxidation of Sulfide to Sulfone

m-CPBA (2 equiv) was added to an ice-cold solution of the sulfide (0.1 mmol) in dry CH_2Cl_2 (5 mL) and stirred overnight under an argon atmosphere. The organic layer was diluted with CH_2Cl_2 (15 mL) and washed with aqueous saturated solutions (15 mL) of sodium bicarbonate, sodium sulfite, and sodium carbonate to make the solution free from *m*-CPBA and *m*-chlorobenzoic acid. The combined organic layer was dried over anhydrous sodium sulfate, which was then removed by filtration. The solvent was removed and the crude mass was purified by column filtration.

General Procedure for Base-Catalyzed Cyclization

The respective sulfone (0.05 mmol) was treated with dry triethylamine (1 equiv) and an excess amount of 1,4-CHD (10 equiv) in $CDCl_3$ (0.5 mL) (for the aromatic sulfones) and in dry benzene (0.5 mL) (for the aliphatic sulfone) for 24 h (unless mentioned). After the completion of the reaction (either monitored by NMR spectroscopy or TLC), the crude product was subjected to flash column chromatography. The product was further purified by HPLC.

*1,4-Bis[2-(3-bromoprop-1-ynyl)phenyl]buta-1,3-diyne (**12**)*

Yellow oil; yield: 91%; ^{1}H NMR (200 MHz): δ = 7.53–7.49 (m, 2H), 7.45–7.40 (m, 2H), 7.32–7.27 (m, 4H, m), 4.22 ppm (s, 4H); ^{13}C NMR (50 MHz): δ = 133.0, 132.3, 129.0, 128.6, 125.6, 124.6, 88.8, 84.7, 81.0, 15.2 ppm.

*Aromatic Sulfide **13***

Brown sticky mass; yield: 79%; ^{1}H NMR (200 MHz): δ = 7.50–7.43 (m, 4H), 7.33–7.29 (m, 4H), 3.78 ppm (s, 4H); ^{13}C NMR (50 MHz): δ = 131.2, 130.2, 128.9, 128.8, 128.0, 125.7, 90.5, 83.4, 81.5, 79.1, 19.7 ppm; MS: *m*/*z*: 309 [*M*+H$^+$]; HRMS: *m*/*z* calcd for $C_{22}H_{12}S$+H$^+$: 309.0735; found: 309.0741.

*Aromatic Sulfone **7***

Yellow solid; yield: 89%; ^{1}H NMR: δ = 7.59 (app d, *J* = 8.8 Hz, 2H), 7.49 (app d, *J* = 8.8 Hz, 2H), 7.40–7.37 (m, 4H), 4.40 ppm (s, 4H); ^{13}C NMR: δ = 132.0, 130.1, 129.0, 128.7, 127.2, 125.7, 85.4, 83.4, 81.2, 79.2, 44.0 ppm; MS: *m*/*z*: 341 [*M*+H$^+$]; HRMS: *m*/*z* calcd for $C_{22}H_{12}O_2S$+H$^+$: 341.063; found: 341.0639.

*Indenyl Sulfone **20***

White solid; yield: 32%; ^{1}H NMR (CD_3COCD_3): δ = 7.79 (d, *J* = 7.2 Hz, 1H), 7.64–7.62 (m, 1H), 7.54–7.47 (m, 3H), 7.37 (d, *J* = 6.8 Hz, 1H), 7.30 (t, *J* = 7.2 Hz, 1H), 7.26–7.21 (m, 2H), 7.15 (s, 1H), 5.33 (s, 2H), 4.46 ppm (s, 2H); ^{13}C NMR: δ = 140.1, 139.8, 137.0, 132.5, 130.6, 129.0, 128.9, 128.8, 126.6, 126.3, 124.1, 123.3, 121.6, 107.3, 101.1, 91.0, 87.7, 82.1, 48.6, 46.5 ppm; MS: *m*/*z*: 343 [*M*+H$^+$]; HRMS: *m*/*z* calcd for $C_{22}H_{14}O_2S$+H$^+$: 343.0789; found: 343.0782.

(4Z,10Z)-1,14-Bis(tetrahydro-2*H*-pyran-2-yloxy)tetradeca-4,10-dien-2,6,8,12-tetrayne (**16**)

White gummy liquid; yield: 91%; ^{1}H NMR (200 MHz): δ = 6.00 (app d, *J* = 12.4 Hz, 2H), 5.90 (d, *J* = 10.8 Hz, 2H), 4.89 (app d, *J* = 3.4 Hz, 2H), 4.48 (d, *J* = 1.6 Hz, 2H), 3.92–3.80 (m, 2H), 3.60–3.50 (m, 2H), 1.83–1.54 ppm (m, 12H); ^{13}C NMR (50 MHz): δ = 122.6, 118.2, 96.8, 94.9, 83.1, 81.1, 80.7, 62.2, 54.6, 30.3, 25.4, 19.1 ppm; MS: *m*/*z*: 379 [*M*+H$^+$]; HRMS: *m*/*z* calcd for $C_{24}H_{26}O_4$+H$^+$: 379.1902; found: 379.1908

(4Z,10Z)-Tetradeca-4,10-dien-2,6,8,12-tetrayne-1,14-diol (**17**)

White sticky mass; yield: 91%; ^{1}H NMR (200 MHz): δ = 5.99 (app d, *J* = 12.2 Hz, 2H), 5.89 (d, *J* = 10.8 Hz, 2H), 4.46 (s, 4H), 2.81 ppm (brs, 2H); ^{13}C NMR (50 MHz): δ = 123.0, 118.5, 97.2, 82.9, 81.4, 80.9, 51.5 ppm; MS: *m*/*z*: 211 [*M*+H$^+$]; HRMS: *m*/*z* calcd for $C_{14}H_{10}O_2$+H$^+$: 211.0756; found: 211.0751

(4Z,10Z)-1,14-Dibromotetradeca-4,10-dien-2,6,8,12-tetrayne (**18**)

Yellow liquid; yield: 90%; ^{1}H NMR (200 MHz): δ = 6.00 (s, 4H), 4.15 ppm (s, 4H); ^{13}C NMR (50 MHz): δ = 122.3, 119.7, 93.6, 83.7, 81.4, 15.0 ppm.

*Aliphatic Sulfide **19***

Brown liquid; yield: 88%; ^{1}H NMR: δ = 6.16 (app d, *J* = 4.4 Hz, 1H), 6.14 (app d, *J* = 4.4 Hz, 1H), 5.98 (d, *J* = 10 Hz, 2H), 3.65 ppm (d, *J* = 2 Hz, 4H); ^{13}C NMR (50 MHz): δ = 126.2, 120.5, 95.8, 85.1, 82.7, 81.3, 20.1 ppm; MS: *m*/*z*: 209 [*M*+H$^+$]; HRMS: *m*/*z* calcd for $C_{14}H_8S$+H$^+$: 209.0423; found: 209.0429.

*Aliphatic Sulfone **8***

Brown sticky liquid; yield: 74%; ^{1}H NMR: δ = 6.28 (d, *J* = 10 Hz, 2H), 6.16 (d, *J* = 10 Hz, 2H), 4.22 ppm (d, *J* = 2 Hz, 4H); ^{13}C NMR: δ = 125.4, 122.6, 86.1 85.7, 85.0, 83.4, 44.7 ppm; MS: *m*/*z*: 241 [*M*+H$^+$]; HRMS: *m*/*z* calcd for $C_{14}H_8O_2S$+H$^+$: 241.0321; found: 241.0331.

*Dibenz-1,1-dioxothiapane **21***

White liquid; yield: 28%; ^{1}H NMR: δ = 7.51–7.49 (m, 8H), 4.02 ppm (s, 4H); ^{13}C NMR: δ = 140.0, 130.9, 129.6, 129.5, 129.1, 128.2, 57.4 ppm; MS: *m*/*z*: 245 [*M*+H$^+$]; HRMS: *m*/*z* calcd for $C_{14}H_{12}O_2S$+H$^+$: 245.0633; found: 245.0641.

*Phenyl Dibenz-1,1-dioxothiapane **22***

White liquid; yield: 4%; ^{1}H NMR (CD_3COCD_3): δ = 7.60–7.55 (m, 4H), 7.35–7.31 (m, 1H), 7.20 (brs, 3H), 7.09 (brs, 3H), 6.81 (d, *J* = 7.2 Hz,

1H), 4.31, 4.28 (AB q, $J=14$ Hz, 2×1H), 4.18 (d, $J=14.4$ Hz, 1H), 3.83 ppm (d, $J=13.6$ Hz, 1H); MS: m/z: 321 [M+H$^+$]; HRMS: m/z calcd for $C_{20}H_{16}O_2S$+H$^+$: 321.0945; found: 321.0941.

Acyclic Sulfone ***1***

White sticky mass; yield: 94%; ^{1}H NMR: $\delta=7.59$–7.57 (m, 4H), 7.54 (d, $J=7.6$ Hz, 2H), 7.44 (d, $J=8.0$ Hz, 2H), 7.36–7.33 (m, 4H), 7.29–7.26 (m, 6H), 4.37 ppm (s, 4H); ^{13}C NMR: $\delta=132.5$, 132.1, 131.8, 128.9, 128.6, 128.3, 128.0, 126.1, 123.7, 122.6, 93.6, 87.5, 86.4, 80.0, 44.0 ppm; MS: m/z: 495 [M+H$^+$]; HRMS: m/z calcd for $C_{34}H_{22}O_2S$+H$^+$: 495.1413; found: 495.1411

Sulfolene ***6***

Yellow liquid; yield: 96%; ^{1}H NMR: $\delta=8.48$ (s, 1H), 7.80 (d, $J=6.8$ Hz, 1H), 7.74–7.72 (m, 1H), 7.67–7.65 (m, 2H), 7.51–7.48 (m, 4H), 7.42–7.36 (m, 5H), 7.31 (dd, $J=3.6$, 1.6 Hz, 1H), 7.20–7.13 (m, 3H), 4.65 (s, 2H), 4.44, 4.16 ppm (AB q, $J=16.4$ Hz, 2H); ^{13}C NMR: $\delta=139.4$, 136.9, 132.9, 132.6, 131.8, 131.6, 131.2, 131.1, 129.9, 129.3, 129.2, 128.7, 128.6, 128.5, 128.4, 128.3, 128.1, 126.9, 126.3, 123.4, 123.2, 122.8, 122.3, 121.0, 94.8, 93.2, 87.1, 86.9, 57.2, 56.1 ppm; MS: m/z: 495 [M+H$^+$]; HRMS: m/z calcd for $C_{34}H_{22}O_2S$+H$^+$: 495.1413; found: 495.1419.

Garratt–Braverman (GB) Product ***32 a***

Colorless solid; yield: 73%; ^{1}H NMR: $\delta=8.31$ (s, 1H), 8.06 (d, $J=8.4$ Hz, 2H), 7.66 (d, $J=8.4$ Hz, 2H), 7.56–7.50 (m, 2H), 7.46 (d, $J=7.2$ Hz, 1H), 7.43–7.37 (m, 1H), 7.26–7.22 (m, 4H), 7.00 (d, $J=8.4$ Hz, 1H), 4.58, 4.52 (AB q, $J=16.0$ Hz, 2H), 4.25, 3.75 (AB q, $J=16.4$ Hz, 2H), 3.70, 3.63 (AB q, $J=18.4$ Hz, 2H), 2.69–2.33 (m, 4H), 2.04–1.96 (m, 2H), 1.78–1.68 ppm (m, 2H); ^{13}C NMR: $\delta=149.5$, 144.7, 140.5, 136.3, 133.9, 132.8, 132.0, 129.3, 129.2, 128.9, 128.7, 127.8, 127.4, 126.4, 125.3, 123.6, 123.5, 122.7, 122.2, 104.1, 86.1, 82.8, 81.6, 57.2, 55.6, 49.4, 38.5, 30.2, 27.1, 20.3 ppm; MS: m/z: 611 [M+H$^+$]; HRMS: m/z calcd for $C_{33}H_{27}N_2O_6S_2$+H$^+$: 611.1311; found: 611.1306.

GB Product ***31 a***

Colorless gummy mass; yield: 25%; ^{1}H NMR: $\delta=8.41$ (d, $J=8.8$ Hz, 2H), 8.33 (s, 1H), 8.00 (d, $J=8.8$ Hz, 2H), 7.61–7.55 (m, 3H), 7.51–7.49 (m, 1H), 7.47–7.41 (m, 2H), 7.37–7.32 (m, 2H), 4.69, 4.60 (AB q, $J=16.0$ Hz, 2H), 4.32, 3.99 (AB q, $J=16.4$ Hz, 2H), 3.30, 3.16 (AB q, $J=16.8$ Hz, 2H), 3.10–3.03 (m, 1H), 3.00–2.94 (m, 1H), 1.85–1.80 (m, 1H), 1.50–1.39 (m, 3H), 0.79–0.75 (m, 1H), 0.26–0.22 ppm (m, 1H); ^{13}C NMR: $\delta=150.3$, 143.9, 140.7, 138.0, 134.1, 133.3, 131.7, 130.3, 130.0, 129.0, 128.8, 128.6, 128.2, 127.7, 126.3, 125.3, 124.7, 123.0, 120.2, 95.5, 92.9, 86.9, 78.3, 57.5, 56.1, 49.8, 41.9, 31.4, 26.4, 19.1 ppm; MS: m/z: 611 [M+H$^+$]; HRMS: m/z calcd for $C_{33}H_{27}N_2O_6S_2$+H$^+$: 611.1311; found: 611.1319.

GB Product ***32 b***

Colorless viscous liquid; yield: 57%; ^{1}H NMR: $\delta=8.19$ (s, 1H), 8.16 (d, $J=8.8$ Hz, 2H), 7.78 (d, $J=8.8$ Hz, 2H), 7.58–7.52 (m, 2H), 7.44–7.37 (m, 2H), 7.28–7.20 (m, 3H), 7.10 (d, $J=8.4$ Hz, 1H), 4.54, 4.50 (AB q, $J=15.6$ Hz, 2H), 4.30, 3.97 (AB q, $J=16.4$ Hz, 2H), 3.81, 3.53 (AB q, $J=18.4$ Hz, 2H), 2.83–2.75 (m, 1H), 2.59–2.43 (m, 3H), 2.06–1.99 (m, 1H), 1.71–1.66 ppm (m, 1H); ^{13}C NMR: $\delta=149.9$, 144.9, 140.6, 136.0, 134.3, 133.5, 132.3, 129.4, 129.2, 128.6, 128.5, 127.6, 126.7, 126.5, 125.6, 123.8, 123.3, 123.1, 122.6. 107.3, 87.2, 85.8, 81.5, 57.2, 55.5, 46.7, 37.4, 30.1, 17.8 ppm; MS: m/z: 597 [M+H$^+$]; HRMS: m/z calcd for $C_{32}H_{25}N_2O_6S_2$+H$^+$: 597.1154; found: 597.1143

GB Product ***31 b***

Colorless liquid; yield: 38%; ^{1}H NMR: $\delta=8.36$ (d, $J=8.4$ Hz, 2H), 8.32 (s, 1H), 8.16 (d, $J=7.6$ Hz, 2H), 7.61 (d, $J=8.4$ Hz, 1H), 7.50 (d, $J=6.8$ Hz, 1H), 7.45–7.30 (m, 4H), 7.30–7.25 (m, 3H), 4.76, 4.67 (AB q, $J=16.0$ Hz, 2H), 4.44, 4.27 (AB q, $J=17.6$ Hz, 2H), 4.28, 4.16 (AB q, $J=16.0$ Hz, 2H), 3.07–2.99 (m, 1H), 1.54–1.04 (m, 1H), 0.96–0.86 ppm (m, 1H); ^{13}C NMR: $\delta=150.1$, 145.1, 141.0, 137.7, 134.2, 133.8, 131.6, 130.3, 129.1, 128.6, 128.5, 128.3, 128.1, 127.2, 126.8, 126.2, 125.1, 124.5, 123.6, 121.2, 97.6, 93.7, 88.9, 78.1, 57.2, 55.8, 53.4, 49.8, 41.3, 29.9, 16.8 ppm; MS: m/z: 597 [M+H$^+$]; HRMS: m/z calcd for $C_{32}H_{25}N_2O_6S_2$+H$^+$: 597.1154; found: 597.1153.

Acknowledgements

D.M. and E.D.J. thank SERC, IISc, and CMSD, University of Hyderabad for computational resources. DST is acknowledged for the J.C. Bose Fellowship grant to E.D.J and for an SERC grant to A.B. that supported this research. R.M. and S.M. are grateful to CSIR, Government of India, for a research fellowship. The NMR spectroscopy and X-ray facility were provided at IIT, Kharagpur by DST under the IRPHA and FIST programmes, respectively. We would also like to thank Mr. L. K. Rajput and Mr. M. K. Sarkar for their help in solving the X-ray structure and to Ms. S. Datta for the densitometric studies.

[1] *Enediyne Antibiotics as Antitumor Agents* (Eds.: D. B. Border, T. W. Doyle), Marcel Dekker, New York, **1995**.
[2] a) A. Basak, S. Mandal, S. S. Bag, *Chem. Rev.* **2003**, *103*, 4077–4094; b) K. Krohn, *Angew. Chem.* **2006**, *118*, 550–553; *Angew. Chem. Int. Ed.* **2006**, *45*, 536–539; c) I. Saito, K. Nakatani, *Bull. Chem. Soc. Jpn.* **1996**, *69*, 3007–3019; d) H. H. Wenk, M. Winkler, W. Sander, *Angew. Chem.* **2003**, *115*, 518–546; *Angew. Chem. Int. Ed.* **2003**, *42*, 502–528; e) M. E. Maier, F. Bosse, A. J. Niestroj, *Eur. J. Org. Chem.* **1999**, 1–13.
[3] a) J. W. Grissom, G. U. Gunawardena, D. Klinberg, D. Huang, *Tetrahedron* **1996**, *52*, 6453–6518; b) P. R. Schreiner, M. Prall, V. Lutz, *Angew. Chem.* **2003**, *115*, 5935–5938; *Angew. Chem. Int. Ed.* **2003**, *42*, 5757–5760.
[4] a) M. W. Perpall, K. P. U. Perera, J. DiMaio, J. Ballato, S. H. Foulger, D. W. Smith, *Langmuir* **2003**, *19*, 7153–7156; b) J. A. John, J. M. Tour, *Tetrahedron* **1997**, *53*, 15515–15534.
[5] P. F. Bross, J. Beitz, G. Chen, X. H. Chen, E. Duffy, L. Kieffer, S. Roy, R. Sridhara, A. Rahman, G. Williams, R. Pazdur, *Clin. Cancer Res.* **2001**, *7*, 1490–1496.
[6] a) R. G. Jones, R. G. Bergman, *J. Am. Chem. Soc.* **1972**, *94*, 660–661; b) R. G. Bergman, *Acc. Chem. Res.* **1973**, *6*, 25–31; c) T. P. Lockhart, R. G. Bergman, *J. Am. Chem. Soc.* **1981**, *103*, 4091–4096; d) K. C. Nicolaou, G. Zuccarello, Y. Oogawa, E. J. Schweiger, T. Kumazawa, *J. Am. Chem. Soc.* **1988**, *110*, 4866–4868.
[7] a) R. Nagata, H. Yamanaka, E. Okazaki, I. Saito, *Tetrahedron Lett.* **1989**, *30*, 4995–4998; b) A. G. Myers, E. Y. Kuo, N. S. Finney, *J. Am. Chem. Soc.* **1989**, *111*, 8057–8059; c) A. G. Myers, P. S. Dragovich, *J. Am. Chem. Soc.* **1989**, *111*, 9130–9132; d) R. Nagata, H. Yamanaka, E. Murahashi, I. Saito, *Tetrahedron Lett.* **1990**, *31*, 2907–2910.
[8] a) M. Schmittel, M. Strittmatter, S, Kiau, *Angew. Chem.* **1996**, *108*, 1952–1954; *Angew. Chem. Int. Ed. Engl.* **1996**, *35*, 1843–1845; b) M. Schmittel, S. Kiau, T. Siebert, M. Strittmatter, *Tetrahedron Lett.* **1996**, *37*, 7691–7694; c) M. Schmittel, J.-P. Steffen, D. Auer, M. Maywald, *Tetrahedron Lett.* **1997**, *38*, 6177–6180; d) M. Schmittel, M. Keller, S. Kiau, M. Strittmatter, *Chem. Eur. J.* **1997**, *3*, 807–816; e) M. Schmittel, M. Strittmatter, S. Kiau, *Tetrahedron Lett.* **1995**, *36*, 4975–4978.
[9] a) S. Braverman, D. Segev, *J. Am. Chem. Soc.* **1974**, *96*, 1245–1247; b) P. J. Garratt, S. B. Neoh, *J. Org. Chem.* **1979**, *44*, 2667–2674; c) Y. S. P. Cheng, P. J. Garratt, S. B. Neoh, V. H. Rumjanek, *Isr. J. Chem.* **1985**, *26*, 101–107; d) S. Braverman, Y. Duar, D. Segev, *Tetrahedron Lett.* **1976**, *17*, 3181–3184; e) Y. Zafrani, H. E. Gottlieb, M. Sprecher, S. Braverman, *J. Org. Chem.* **2005**, *70*, 10166–10168.
[10] A. M. Maxam, W. Gilbert, *Methods Enzymol.* **1980**, *65*, 499–560.
[11] A. Basak, S. Das, D. Mallick, E. D. Jemmis, *J. Am. Chem. Soc.* **2009**, *131*, 15695–15704.
[12] M. Schmittel, M. Strittmatter, K. Vollmann, S. Kiau, *Tetrahedron Lett.* **1996**, *37*, 999–1002.
[13] a) C. Glaser, *Annalen der Chemie und Pharmacie* **1870**, *154*, 137–171; b) A. S. Hay, *J. Org. Chem.* **1962**, *27*, 3320–3321.

[14] The absence of 1,4-CHD led to the decomposition of starting material. However, no GB product could be isolated.
[15] CCDC 776535 and CCDC 826450 contain the supplementary crystallographic data for this paper. These data can be obtained free of charge from the Cambridge Crystallographic Data Centre via www.ccdc.cam.ac.uk/data_request/cif.
[16] S. Kotha, P. Khedkar, A. K. Ghosh, *Eur. J. Org. Chem.* **2005**, *16*, 3581–3585.
[17] The formation of product **21** could also be explained by stepwise double Bergman cyclization (BC). However, because of the large ring size (15-membered before cyclization and 11-membered after first BC) and also the requirement of basic conditions to carry out the cyclization, such a process can be ruled out.
[18] M. F. Semmelhack, T. Neu, F. Foubelo, *J. Org. Chem.* **1994**, *59*, 5038–5047.
[19] a) All computations were performed using the Gaussian 09 package. The nature of the stationary points was characterized by vibrational frequency calculations; b) Gaussian 09, Revision A.02, M. J. Frisch et al. Gaussian, Inc., Wallingford, CT, **2009**. The 6-31+G* basis set was used for all the calculations.
[20] Y. Zhao, D. G. Truhlar, *Theor. Chem. Acc.* **2008**, *120*, 215–241.
[21] a) A. D. Becke, *J. Chem. Phys.* **1993**, *98*, 5648–5652; b) A. D. Becke, *Phys. Rev. A* **1988**, *38*, 3098–3100; c) C. Lee, W. Yang, R. G. Parr, *Phys. Rev. B* **1988**, *37*, 785–789; d) S. H. Vosko, L. Wilk, M. Nusair, *Can. J. Phys.* **1980**, *58*, 1200–1211.
[22] W. Hehre, L. Radom, P. von R. Schleyer, J. A. Pople, *Ab Initio Molecular Orbital Theory*, Wiley, New York, **1986**.
[23] For computations on cyclization of eneyneallenes, see: a) P. R. Schreiner, A. Navarro-Vázquez, M. Prall, *Acc. Chem. Res.* **2005**, *38*, 29–37; b) F. Stahl, D. Moran, P. v. R. Schleyer, M. Prall, P. R. Schreiner, *J. Org. Chem.* **2002**, *67*, 1453–1461; c) M. Schmittel, J.-P Steffen, M. A. W. Angel, B. Engels, C. Lennartz, M. Hanrath, *Angew. Chem.* **1998**, *110*, 1633–1635; *Angew. Chem. Int. Ed.* **1998**, *37*, 1562–1564; d) B. Engels, C. Lennartz, M. Hanrath, M. Schmittel, M. Strittmatter, *Angew. Chem.* **1998**, *110*, 2067–2070; *Angew. Chem. Int. Ed.* **1998**, *37*, 1960–1963; e) B. Engels, M. Hanrath, *J. Am. Chem. Soc.* **1998**, *120*, 6356–6361.
[24] J. Gräfenstein, E. Kraka, M. Filatov, D. Cremer, *Int. J. Mol. Sci.* **2002**, *3*, 360–394.

Received: November 3, 2011
Published online: March 7, 2012

